Diagnosing Microscopic Blood Samples for Early Detection of Leukemia by Deep and Hybrid Learning Techniques

Ebrahim Mohammed Senan[1(✉)], Mukti E. Jadhav[2], Ramesh R. Manza[1], and Vandana Bagal[3]

[1] Department of Computer Science and Information Technology, Dr. Babasaheb Ambedkar Marathwada University, Aurangabad, India
senan1710@gmail.com
[2] Shri Shivaji Science and Arts College, Chikhli District, Buldana, India
[3] K.K. Wagh Institute of Engineering Education and Research, Nasik, India

Abstract. Blood is an important component of the human, which consists of many important components including White Blood Cells (WBC). Leukaemia is one of the dangerous kinds of cancer that affect the blood and bone marrow, affecting children and adults. Acute lymphoblastic Leukaemia (ALL) is dangerous and deadly type of blood cancer. Hematologists and experts work on diagnosing blood by taking patient samples and analyzing them with a high-quality magnifying lens. However, manual diagnosis is boring, time-consuming, and more prone to errors and differing expert views. Therefore, artificial intelligence techniques solve this problem and support the opinions of highly experienced experts. This research aims to develop diagnostic systems using a Convolutional Neural Network (CNN) and a hybrid CNN and SVM to diagnose the ALL_IDB2 dataset for early diagnosis of Leukaemia. CNN models and a hybrid technique consisting of two blocks were implemented, the first block of CNN models to extract feature and the second block, the SVM algorithm, to classify the feature. All the proposed systems achieved superior results in diagnosing the ALL_IDB2 dataset for early diagnosis of Leukaemia.

Keywords: ALL · Machine learning · CNN · Hybrid method

1 Introduction

Blood is one of the critical components of the human body, and it is the dynamo that moves the human. Blood comprises several elements, namely plasma 55%, RBC 45%, WBC and platelets less than 1% [1]. Plasma transports minerals, hormones, proteins and other nutrients through blood vessels and gets rid of harmful elements in the form of waste products. Blood is produced in the bone marrow, the soft tissue within the bony cavity. When there is overactive or abnormal bone marrow [2], it produces immature cells or multicolored cells. Hematology is diagnosed by extracting WBC information

R. Manza et al. (Eds.): ACVAIT 2022, AISR 176, pp. 23–38, 2023.
https://doi.org/10.2991/978-94-6463-196-8_4

[3]. The diagnosis is made based on increased WBC with immature myeloid or lymphoid cells, low platelets and neutrophils [4]. Therefore, hematologists analyze blood samples under a microscope to diagnose and identify blast cells. Thus, the presence of blast cells in blood smears is one of the most critical symptoms of Leukaemia. There are some types of Leukaemia, the most dangerous of which is ALL. ALL is considered one of the most dangerous and deadly types, prevalent in children and adults. Early diagnosis of Leukaemia and its types is essential for timely treatment. Diagnosis by blood smears and microscopic blood tests is one of the methods that accelerate the detection of Leukaemia without medical risks [5]. There are also many techniques for diagnosing Leukaemia, such as interventional radiology, biopsy, percutaneous aspiration, catheter drainage and other methods that have limitations for the sensitivity of the technique [6]. There are also techniques such as molecular cytogenetics, array-based comparative genetic hybridization (aCGH) and long-distance reverse transcription-polymerase chain reaction (LDI-PCR) that require highly experienced hematologists, time and extensive work to diagnose Leukaemia [7]. There is also a similarity in the characteristics of normal cells and lymphocytes in their early stages, which are challenges for the early diagnosis. Therefore, lymphocytes were categorised into some types: normal, reactive, and atypical. Thus, each type has characteristics that distinguish it from the other type. Since the diagnosis is completed manually, it is a boring and time-consuming method and prone to many errors. Therefore, automated diagnosis using artificial intelligence techniques is essential in the early diagnosis of Leukaemia. Several researchers have proposed automated methods for the early diagnosis of Leukaemia by extracting chromatic, morphological, and texture characteristics from WBC micrographs. Therefore, the diagnosis of microscopic blood sample data set by deep and machine learning techniques will lead to an accurate, reliable and rapid diagnosis of early detection of Leukaemia. CNN models have the ability to solve the deficiencies of manual diagnosis and their excellent ability to differentiate normal and abnormal cells (blast cells). This study focuses on the diagnosis of the ALL_IDB2 dataset; extracting feature and diagnosing them using CNN models, hybrid techniques between CNN models, and machine learning algorithms (SVM).

The significant contributions in this study are as follows:

- Noise and all artifacts were removed using overlapping filters.
- Increasing the dataset images by using the data augmentation method.
- Adjust the parameters of CNN models to extract deep features with accurateness and efficiency.
- Applied a hybrid technique between CNN models and SVM algorithm to obtain superior results for early detection of Leukaemia.

The rest of the article is arranged as follows: Sect. 2 presents a group of related work. Section 3 describes the methods and techniques used to analyze and classify a data set. Section 4 presents the results execution of the systems. Section 5 offers a discussion of the systems. Concludes the work in Sect. 6.

2 Related Work

This section reviews many previous studies related to the diagnosis of microscopic images of microscopic blood samples for the early detection of Leukaemia. CNN and SVM help diagnose microscopic images and identify Leukaemia.

Nizar et al. presented the CNN and machine learning techniques to diagnose the ALL-IDB Image Bank datasets to detect Leukaemia subtypes. The data augmentation method to obtain images was also applied artificially. The CNN got an accuracy of 81.74% [8]. Goutam et al. proposed a model consisting some stages: preprocessing, region of interest, extraction of features, and classification stage for classifying microscopic blood samples. Feature extraction based on Local Directional path (LDP) and feature classification by SVM, which achieved superior results for the classification of microscopic images [9]. Rawat et al. presented a method for diagnosing lymphoid and myeloid cells for the giagnosis of Leukaemia. The system optimizes the images of the AML and ALL datasets and extracts 331 features textures, geometrics, and chromaticities to distinguish between normal and malignant cells. The features were classified by SVM, which achieved good results for classifying the two data sets [10]. Amin et al. discuss an approach to discovering lymphocytic Leukaemia. All dataset images were enhanced, WBC was extracted using k-means, then statistical and geometrical features were extracted from WBC. The features were classified by the SVM algorithm, which got an accuracy of 97% [11]. Zhana et al. proposed two approaches; the first approach is to separate WBCs from the rest of the cells, and the second approach is to extract the most critical geometrical, statistical, and shape features and transform the discrete cosine. The result of systems on the ALL-IDB data set, and it achieved an accuracy of 97.45% [12]. Cecilia et al. presented a new approach to identify WBC from images of the ALL-IDB dataset to diagnose them as normal or leukemic. All images passed through the stages of enhancement, segmentation, WBC recognition and classification; the system achieved an accuracy of 99.7% [13]**.** Nizar et al. offered a method for diagnosing Leukaemia subtypes using CNN models and machine learning. The data augmentation has been used to augment the images. All models performed well, as the performance of the CNN was more useful than the machine learning algorithms, which reached an accuracy of 88.25 [8]. Aqsa et al. presented a method to detect Leukaemia in its early stages. A color filter was applied to detect white blood cells, and then a wavelet and curvelet descriptor was used to extract structural features. Then feature classification by KNN and SVM algorithms has yielded promising results [14]**.** Rawat et al. presented a novel method for diagnosing lymphocytes by first isolating white blood cells from other blood cells. The GLCM extracted the texture and shape features algorithm and classified by the SVM classifier. When diagnosing texture features, the system got an accuracy of 86.7%, while the system got an accuracy of 56.1% with shape features [15]. Lakshmi et al. offered a method for early diagnosis of Leukaemia. They applied the K-means clustering to cluster the lesion and isolated it from the rest of the cells. The diagnosis was made using the SVM algorithm, which got an accuracy of 95% [16].

3 Materials and Methods

In this section, the most critical strategies and materials for analyzing and classifying the ALL_IDB2 data set as described in Fig. 1. All images have been enhanced to remove noise and obtain high efficiency in the following stages. After the improvement process, two proposed systems were applied. The first system through two CNN models. The second system is a hybrid between CNN with SVM.

3.1 Description of Two Datasets

All the systems presented were evaluated using the publicly available ALL-IDB dataset using the machine, deep learning, and a fusion them. The publicly available dataset contains images of microscopic blood samples for ALL and normal images. The data set focused on ALL, which were more severe and lethal than other types. Lymphomas were classified and identified for each image by specialized experts. All images were acquired by a Canon PowerShot G5 optical microscope and RGB color at a high-resolution of 1944 x 2592 pixels. This data set consists of ALL_IDB1 and ALL_IDB2; each image contains approximately 39,000 blood cells. This study targets the ALL_IDB2 dataset, which includes 260 images equally divided into 130 images of malignant and 130 normal blood cells [17]. Figure 2.a describes a set of samples for the data set.

3.2 Pre-processing

The data set images were fed before applying the enhancement process; because of the noise and lack of image contrast, the performance of the proposed systems was inaccurate. Thus, all dataset images were enhanced before feeding them into deep learning models [18]. The first step in biomedical image processing is to remove unwanted noise and artifacts. When analyzing blood samples under the microscope, there are light reflections, in addition to liquid samples that are placed with the blood sample, all of which affect the performance of artificial intelligence techniques. Thus, applying filters to enhance the images is required to obtain high performance in the later stages of image processing [19]. In this study, the images were optimized using two filters. First, an

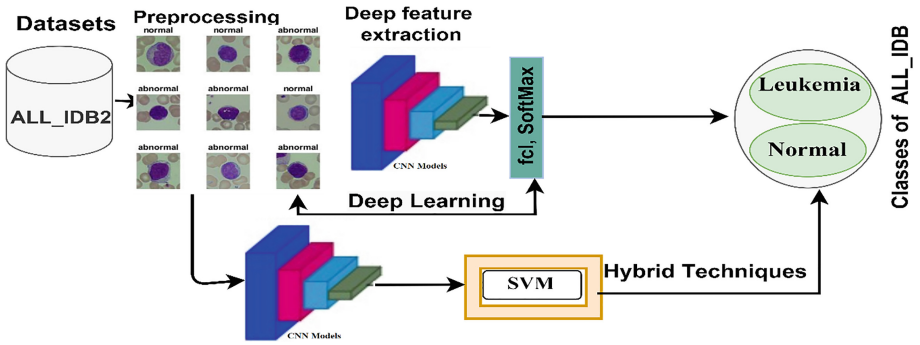

Fig. 1. Methodology for diagnosing the ALL_IDB2 dataset.

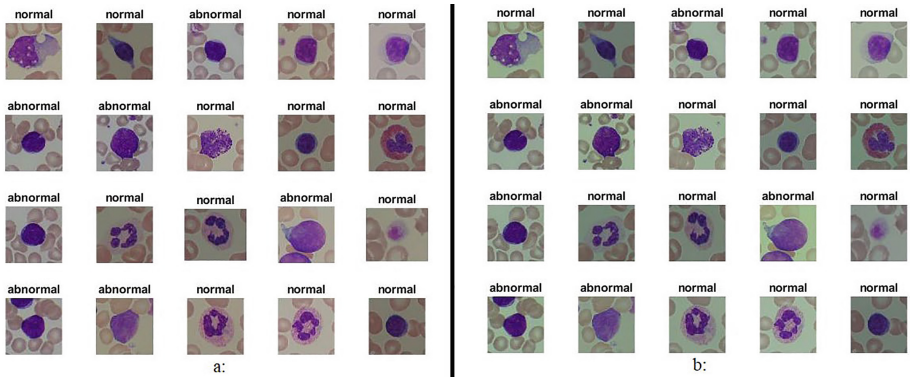

Fig. 2. A set of data set samples before and after enhancement (a) ALL-IDB2 samples and (b) Enhanced ALL-IDB2 dataset images.

average filter is used to improve the contrast of the images. The filter size is set to 7*7 so that the filter replaces each goal pixel by an average of 48 neighbouring pixels, and the process continues for each image pixel. Equation 1 shows how the average filter works [20].

$$z(n) = \frac{1}{N}\sum_{i=0}^{M-1} y(n-1) \tag{1}$$

where *z(n)* refers to input, *y(n-1)* refers to earlier input and *N* is the pixels numbers.

Second, a Laplacian filter was used to detect white blood cells' edges. Equation 2 defines the technique of action of the filter.

$$\nabla^2 f = \frac{\partial^2 f}{\partial^2 x} + \frac{\partial^2 f}{\partial^2 y} \tag{2}$$

differential equation of second order is $\nabla^2 f$ and *x, y* are the location of the matrix.

Finally, the system produces an improved image using subtracting the images produced by the Laplacian method from the image produced using the average method. Equation 3 describes the final step of producing an enhanced image.

$$EN = z(m) - \nabla^2 f \tag{3}$$

where *EN* represents the enhanced image

Figure 2.b represents set of images after the enhancement process.

3.3 Convolutional Neural Networks (CNN)

The CNN are called deep learning and have the superior ability to classify, and recognize patterns. CNN work in many fields, such as motion modelling, speech recognition, object segmentation, and biomedical image processing. CNN contain many 2D layers and are suitable for processing and diagnosing 2D images. CNN models differ in the number of layers and the weights of each layer [21]. The work of filters is to convolute around the

image to be handle. In each layer, neurons receive associations from the earlier layers and neurons of the same layer. The core of CNN's work is to represent the input images at many levels; To classify images, layers amplify aspects of the most important features and suppress unimportant (irrelevant) differences. Figure 3 shows the architecture for the AlexNet and ResNet-18 [22]. Where layers work on specific processing of images, for example, the first layer detects the edges of the image, the second layer for extracting the geometric features, the third layer extracts the features of texture and shape, and so on. As described in Fig. 3, networks consist of the following most important layers:

- Convolutional Layer: The number of convolutional layers differs from model to another. The name CNN comes from the name of the Convolutional Layer. The convolutional layer is one of the major layers in CNN, and the convolution process is implemented between the filter w (t) and the image to be processed x (t). The mechanism is done as described in Eq. 4. Three critical parameters that define and control the work of convolutional layers are the size of the filter, p-step and zero padding. The larger the size of the filter, will more the filter wrap around the image, while zero-padding keeps the original image size. The p-step operates to specify the number of filter steps on the image [24].

$$s(t) = (\mathrm{x} * \mathrm{w})(\mathrm{t}) = \int x(a)w(t-a)da \tag{4}$$

- pooling Layer: This layer reduces the resulting dimensions of the convolutional layer. There are two types of this layer: Max and Average Pooling. Max-Pooling specifies the max pixel from the pixels specified by a filter and represents it in the following stages [25]. Average-Pooling calculates the average weight of the weights set by the filter and represents all values by their average value.
- Fully Connected Layer (FCL): This layer contains millions of interconnected neurons responsible for classifying the input images. It works to convert feature maps from binary representation to mono representation.
- There are also many auxiliary layers, such as the ReLU (Rectified Linear Unit) layer, which comes after the convolutional layers and works to handle positive weights, suppress negative weights, and convert them to zero as explained in the Eq. 5. CNN models produce millions of parameters, which causes overfitting, so the dropout layer solves this problem by setting it to, say, 50%, which means 50% of neurons are passed in each iteration, but one of the disadvantages is that it doubles the training time [26]

$$\mathrm{ReLU(x)} = \begin{cases} x, x \geq 0 \\ 0, x < 0 \end{cases} \tag{5}$$

.

- Finally, the Softmax activation layer works to classify each input image into its appropriate class. In this work, the Softmax function will produce two neurons that are either Leukaemia or normal according to the data set classes.

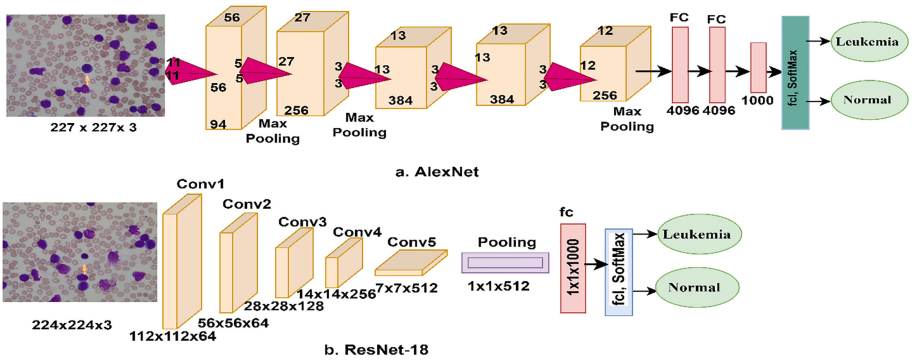

Fig. 3. Structure of a. AlexNet and b. ResNet-18.

3.4 Hybrid of Deep and Machine Learning

This section presents a hybrid method of CNN models and SVM for the diagnosis of Leukaemia. CNN models require high specification computer resource specifications to train the data set, and it takes a long time to train the data set, so these hybrid techniques solve this challenge [26]. The technique removes Fully Connected Layer from the CNN model and replaces them with the SVM algorithm. In this section, the hybrid approach consists of two blocks: the firstly is AlexNet and ResNet-18 models to extract the deep feature [27]. Secondly is the SVM classifier for classifying deep features. Figures 4a and b show the hybrid architecture. The SVM algorithm replaces the fully connected layer of deep learning models.

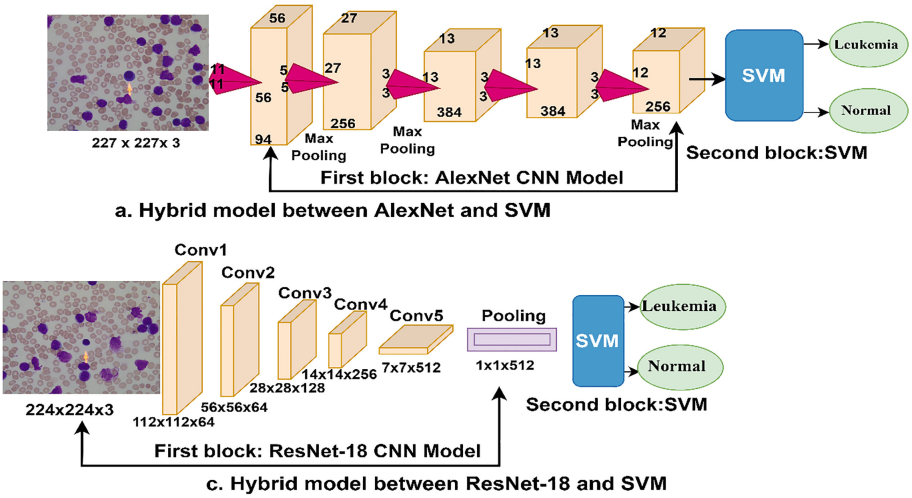

Fig. 4. Hybrid technique a. AlexNet + SVM and b. ResNet-18 + SVM.

Table 1. Splitting the ALL_IDB2 datasets

Phase	training and validation		Testing (20%)
Classes	Training (80%)	validation (20%)	
Leukaemia	83	21	26
Normal	83	21	26

4 Experimental Result

4.1 Splitting Dataset

All proposed systems in this work were evaluated on the ALL_IDB2 dataset that contains 260 images equally divided into two classes, Leukaemia and normal. The data set has been split into 80% for training and validation (80:20, respectively) and 20% for testing. Table 1 describes the splitting of the ALL_IDB2 data set through stages of the training, validation, and testing systems (Leukaemia and normal). The systems were executed on the MATLAB 2018b executable environment and implemented on a computer with Intel ® i5 a 6th generation, GPU of 4 GB, and RAM of 12 GB.

4.2 Evaluation Metrics

In this section, we explain the appropriate statistical measures that evaluate the performance of the networks implemented in this study, whether deep learning models or hybrid method on the ALL_IDB2 dataset for early diagnosis of Leukaemia. Equations 6, 7, 8, 9 and 10 show the most critical measures that evaluate the performance of systems. Each network produced a confusion matrix from which to obtain information for the equations. The confusion matrix includes all correctly classified images named TP and TN and incorrectly classified images named FP and FN [28].

$$\text{Accuracy} = \frac{\text{TN} + \text{TP}}{\text{TN} + \text{TP} + \text{FN} + \text{FP}} * 100\% \tag{6}$$

$$\text{Precision} = \frac{\text{TP}}{\text{TP} + \text{FP}} * 100\% \tag{7}$$

$$\text{Sensitivity} = \frac{\text{TP}}{\text{TP} + \text{FN}} * 100\% \tag{8}$$

$$\text{Specificity} = \frac{\text{TN}}{\text{TN} + \text{FP}} * 100\% \tag{9}$$

$$\text{AUC} = \frac{\text{TruePositiveRate}}{\text{FalsePositiveRate}} = \frac{\text{Sensitivity}}{\text{Specificity}} \tag{10}$$

where:

The true positive (TP) denotes the number of Leukaemia images which correctly classified.

True negative (TN) means the number of normal images which correctly classified.

A false positive (FP) describes the number of normal images incorrectly categorised as Leukaemia.

False negatives (FN) represent the number of Leukaemia images incorrectly categorised as normal.

4.3 CNN Models Results

In this section, the evaluation results of CNN models based on transfer learning are AlexNet and ResNet-18 on the ALL_IDB2 dataset. The dataset contains a small number of images, which affects the accuracy of the diagnosis because CNN models need a large number of images. Thus, a data augmentation technique was used, in which the images artificially increased. There are many operations performed by the image augmentation technique, such as rotation in many angles, shifting, flipping, and other operations [29].

Table 2 describes the tuning of AlexNet and ResNet-18 models. The optimizer "adam" is set for both models and the setting of Max Epochs, Validation Frequency, Mini Batch Size, and Execution Environment.

Table 3 illustrates the results of both AlexNet and ResNet-18, where it is noted that ResNet-18 outperforms the AlexNet model for classifying the ALL_IDB2 dataset. The ResNet-18 model achieved an accuracy of 97.4%, a precision, sensitivity, specificity of 97.5% for all measures, and an AUC of 97.44%. In contrast, the AlexNet model got accuracy, precision, sensitivity, specificity, and AUC with a percentage of 96.2%, 96.5%, 96%, 96%, and 98.82%, respectively.

Figure 5 displays the execution of AlexNet and ResNet-18 for classifying the ALL_IDB2 dataset for diagnosis of Leukaemia.

Figure 6 illustrates the confusion matrix created by the AlexNet and ResNet-18 models for diagnosing ALL_IDB2 dataset for detection of Leukaemia. The confusion matrix includes all rightly classified dataset images represented by the primary diameter called TP and TN and inaccurately classified represented by the secondary diameter FP and FN. Figure 6.a shows the confusion matrix for AlexNet, which reached an overall accuracy of 96.2%, an accuracy of 100% for diagnosing Leukaemia samples,

Table 2. Tuning training options for AlexNet and ResNet-18 models

Options	AlexNet	ResNet-18
training Options	adam	Adam
Mini Batch Size	128	15
Max Epochs	10	4
Initial Learn Rate	0.0001	0.0001
Validation Frequency	50	5
Execution Environment	4 GB GPU	4 GB GPU

Table 3. The results of the CNN models

Measure	AlexNet	ResNet-18
Accuracy %	96.2	97.4
Precision %	96.5	97.5
Sensitivity %	96	97.5
Sepecificy %	96	97.5
AUC %	98.82	97.44

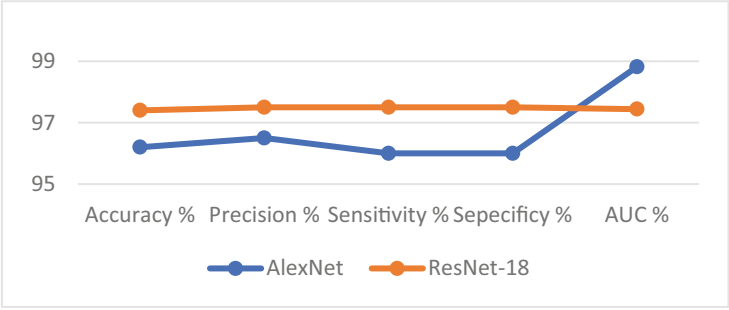

Fig. 5. Display execution of CNN models for classifying the ALL_IDB2 images.

and an accuracy of 92.3% for diagnosing normal images. While Fig. 6.b describes the confusion matrix of ResNet-18, which reached an overall accuracy of 97.4%, an accuracy of 94.9% for diagnosing Leukaemia samples, and an accuracy of 100% for diagnosing normal blood samples.

4.4 Results of the Hybrid CNN with SVM Algorithm

This section reviews the performance results of hybrid technologies between AlexNet and ResNet-18 and SVM machine learning. These techniques worked to overcome the challenges in machine learning models related to their demand for high-performance computer specifications. They are taking a long time to train the data set. This technique consists of CNN for feature map extraction and the SVM for classification. Hybrid techniques have achieved superior results for diagnosing Leukaemia dataset.

Table 4 presents the results of the AlexNet + SVM and ResNet-18 + SVM hybrid technologies. It is noted that these techniques have achieved superior results for the detection of Leukaemia. It is noted that ResNet-18 + SVM has slightly outperformed AlexNet + SVM. The AlexNet + SVM network achieved an accuracy of 98.1% and an equal ratio of accuracy, sensitivity, specificity by 98% for all measures. While ResNet-18 + SVM network achieved an accuracy of 98.7% and an equal percentage of precision, sensitivity, specificity by 98.5% for all measures.

Figure 7 displays hybrid technique performance.

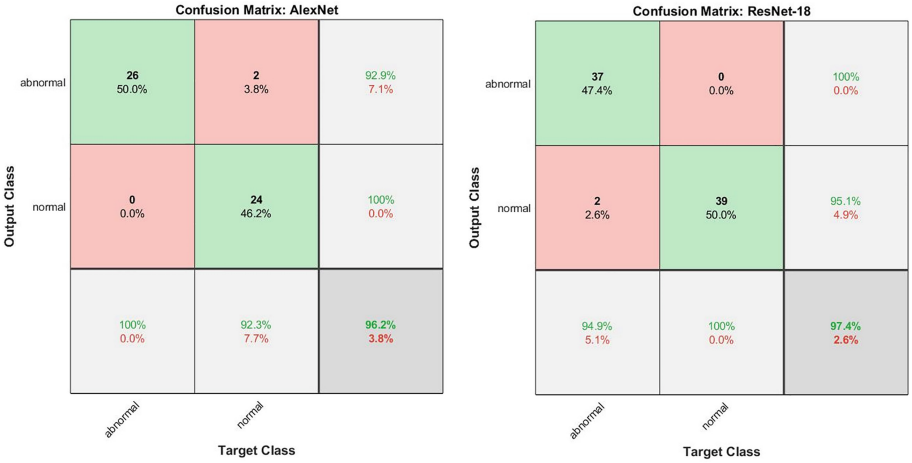

Fig. 6. Confusion matrix for diagnosing ALL_IDB2 data sets (a): AlexNet and (b): ResNet-18

Table 4. The results of the hybrid models on the ALL_IDB2 datasets

Measure	AlexNet + SVM	ResNet-18 + SVM
Accuracy %	98.1	98.7
Precision %	98	98.5
Sensitivity %	98	98.5
Sepecificy %	98	98.5

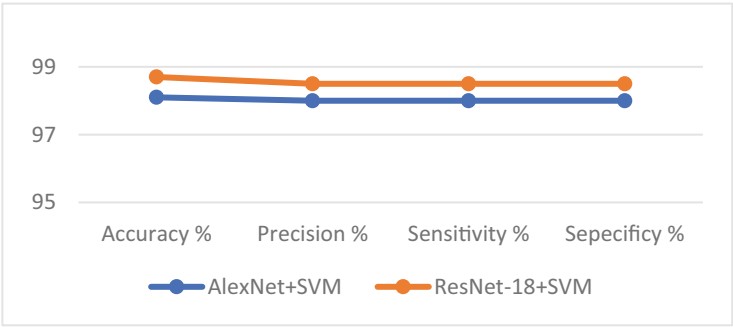

Fig. 7. Displays the performance of the hybrid techniques.

Figure 8a and b describe the confusion matrix produced by AlexNet + SVM and ResNet-18 + SVM hybrid technologies, respectively, to classify the ALL_IDB2 dataset for early diagnosis of Leukaemia. AlexNet + SVM achieved an overall accuracy of

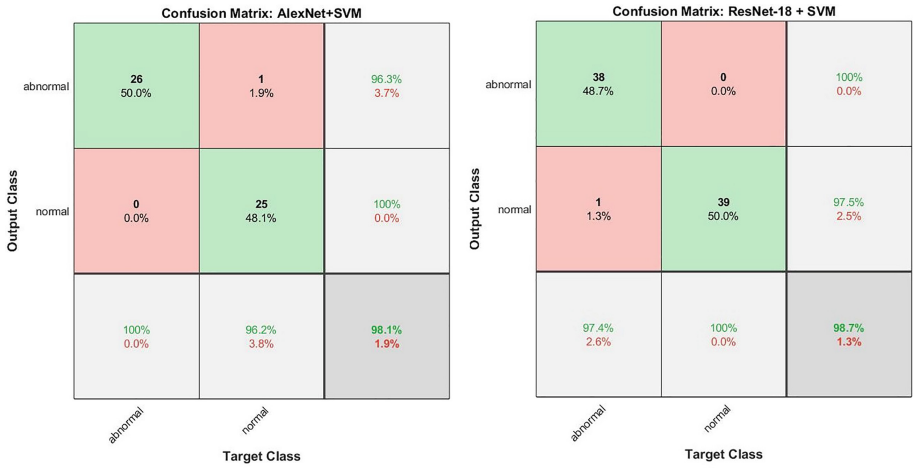

Fig. 8. Confusion matrix for diagnosing ALL_IDB2 data sets (a): AlexNet + SVM and (b): ResNet-18 + SVM

98.1%, an accuracy of 100% for diagnosing Leukaemia, and 96.2% for diagnosing normal blood samples. In contrast, ResNet-18 + SVM reached an overall accuracy of 98.7%, an accuracy of 97.4% for diagnosing Leukaemia, and 100% for diagnosing normal blood samples.

5 Discussion

This section discusses the proposed systems in this paper. Four proposed systems are two CNN models and two-hybrid technologies to classify the ALL_IDB2 dataset for early detection of Leukaemia. All dataset images were subjected to optimization to remove artifacts. A data augmentation method was used to avoid overfitting. The first proposed system is two CNN models based on the transfer learning method, AlexNet and ResNet-18, the two models, have achieved excellent results. AlexNet got an accuracy of 96.2%, while ResNet-18 achieved an accuracy of 97.4%. The second proposed system is two hybrid networks between deep learning and the SVM algorithm. The two networks achieved superior results, with AlexNet + SVM achieving an accuracy of 98.1%, while ResNet-18 + SVM achieved 98.7%.

Table 5 outlines the results of the proposed systems performed on the ALL_IDB2 dataset. First, AlexNet and AlexNet + SVM achieved the best performance and reached 100% accuracy for classifying leukaemia images. Second, for normal class, both ResNet-18 and ResNet-18 + SVM reached 100% accuracy. The table shows that the hybrid systems between CNN and SVM models have better results than CNN models, and this is one of our main contributions in this study.

Figure 9 illustrates the execution of all the proposed systems for classifying each class in the data set.

Table 5. Accuracy of each system in diagnosing each class

Diseases	Deep learning		Hybrid	
	Alex-Net	Res-Net-18	AlexNet + SVM	ResNet-18 + SVM
Leukaemia	100	94.9	100	97.4
Normal	92.3	100	96.2	100

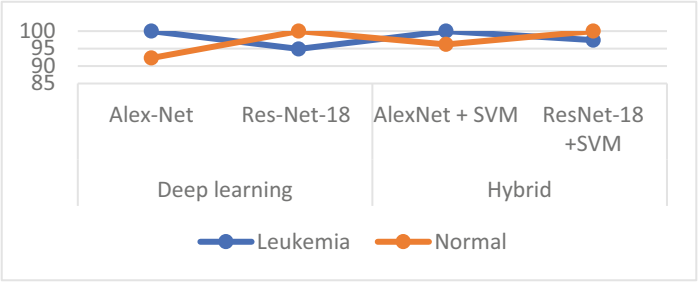

Fig. 9. Display the implementation of the systems for each class in the data set.

6 Conclusion

Artificial intelligence techniques in the medical sector have helped the challenges in manual diagnosis represented by the shortcomings of manual diagnosis, and the taking a long time to track images. Deep and automated learning techniques are considered highly efficient analytical and diagnostic tools. In this study, four different networks were developed between two CNN are AlexNet and ResNet-18, and extracting deep features. Two-hybrid networks between CNN and SVM consist of two blocks, firstly, the CNN model to extract deep features. The secondly deep feature map diagnosis is SVM. All systems have achieved outstanding results, and the superiority of hybrid techniques over CNN models is noted.

Data Availability. In this work, the data were collected from the dataset ALL_IDB2 used to support the results of this work: https://www.kaggle.com/nikhilsharma00/leukemia-dataset.

Conflicts of Interest. No conflict of interest among the authors.

References

1. D. H. Kuan, C. C. Wu, W. Y. Su, and N. T. Huang, A Microfluidic Device for Simultaneous Extraction of Plasma, Red Blood Cells, and On-Chip White Blood Cell Trapping, Scientific Reports 2018 8:1, vol. 8, no. 1, pp. 1–9, Oct. 2018, doi: https://doi.org/10.1038/s41598-018-33738-8.
2. C. L. Sawyers, C. T. Denny, and O. N. Witte, Leukemia and the disruption of normal hematopoiesis, Cell, vol. 64, no. 2, pp. 337–350, Jan. 1991, doi: https://doi.org/10.1016/0092-8674(91)90643-D.

3. S. Agaian, M. Madhukar, and A. T. Chronopoulos, Automated screening system for acute myelogenous leukemia detection in blood microscopic images, IEEE Systems Journal, vol. 8, no. 3, pp. 995–1004, 2014, doi: https://doi.org/10.1109/JSYST.2014.2308452.
4. C. Haworth, A. D. Heppleston, P. H. Morris Jones, R. H. Campbell, D. I. Evans, and M. K. Palmer, Routine bone marrow examination in the management of acute lymphoblastic leukaemia of childhood., Journal of Clinical Pathology, vol. 34, no. 5, pp. 483–485, May 1981, doi: https://doi.org/10.1136/JCP.34.5.483.
5. N. Patel and A. Mishra, Automated Leukaemia Detection Using Microscopic Images, Procedia Computer Science, vol. 58, pp. 635–642, Jan. 2015, doi: https://doi.org/10.1016/J.PROCS.2015.08.082.
6. K. M. Garrett Kevin M., F. A. Hoffer, F. G. Behm, K. W. Gow, M. M. Hudson, and J. T. Sandlund, Interventional radiology techniques for the diagnosis of lymphoma or leukemia, Pediatric Radiology 2002 32:9, vol. 32, no. 9, pp. 653–662, Jul. 2002, doi: https://doi.org/10.1007/S00247-002-0743-2.
7. T. S. K. Wan, Cancer Cytogenetics: Methodology Revisited, Annals of Laboratory Medicine, vol. 34, no. 6, pp. 413–425, Oct. 2014, doi: https://doi.org/10.3343/ALM.2014.34.6.413.
8. N. Ahmed, A. Yigit, Z. Isik, and A. Alpkocak, Identification of Leukemia Subtypes from Microscopic Images Using Convolutional Neural Network, Diagnostics 2019, Vol. 9, Page 104, vol. 9, no. 3, p. 104, Aug. 2019, doi: https://doi.org/10.3390/DIAGNOSTICS9030104.
9. D. Goutam and S. Sailaja, Classification of acute myelogenous leukemia in blood microscopic images using supervised classifier, ICETECH 2015 - 2015 IEEE International Conference on Engineering and Technology, Sep. 2015, doi: https://doi.org/10.1109/ICETECH.2015.7275021.
10. J. Rawat, A. Singh, B. HS, J. Virmani, and J. S. Devgun, Computer assisted classification framework for prediction of acute lymphoblastic and acute myeloblastic leukemia, Biocybernetics and Biomedical Engineering, vol. 37, no. 4, pp. 637–654, Jan. 2017, doi: https://doi.org/10.1016/J.BBE.2017.07.003.
11. M. M. Amin, S. Kermani, A. Talebi, and M. G. Oghli, Recognition of Acute Lymphoblastic Leukemia Cells in Microscopic Images Using K-Means Clustering and Support Vector Machine Classifier, Journal of Medical Signals and Sensors, vol. 5, no. 1, p. 49, Jan. 2015, doi: https://doi.org/10.4103/2228-7477.150428.
12. Z. F. Mohammed and A. A. Abdulla, An efficient CAD system for ALL cell identification from microscopic blood images, Multimedia Tools and Applications 2020 80:4, vol. 80, no. 4, pp. 6355–6368, Oct. 2020, doi: https://doi.org/10.1007/S11042-020-10066-6.
13. C. di Ruberto, A. Loddo, and G. Puglisi, Blob Detection and Deep Learning for Leukemic Blood Image Analysis, Applied Sciences 2020, Vol. 10, Page 1176, vol. 10, no. 3, p. 1176, Feb. 2020, doi: https://doi.org/10.3390/APP10031176.
14. A. Jabeen, S. Jabeen, S. A. Shah, and W. A. Rao, Efficient Features for Effectively Detection of Leukemia Cells, Proceedings - 2020 23rd IEEE International Multi-Topic Conference, INMIC 2020, Nov. 2020, doi: https://doi.org/10.1109/INMIC50486.2020.9318085.
15. J. Rawat, A. Singh, H. S. Bhadauria, and J. Virmani, Computer Aided Diagnostic System for Detection of Leukemia Using Microscopic Images, Procedia Computer Science, vol. 70, pp. 748–756, Jan. 2015, doi: https://doi.org/10.1016/J.PROCS.2015.10.113.
16. V. L. Thanmayi A, S. D. Reddy, and S. Kochuvila, Detection of Leukemia Using K-Means Clustering and Machine Learning, Lecture Notes of the Institute for Computer Sciences, Social-Informatics and Telecommunications Engineering, LNICST, vol. 383, pp. 198–209, Mar. 2021, doi: https://doi.org/10.1007/978-3-030-79276-3_15.
17. R. D. Labati, V. Piuri, and F. Scotti, All-IDB: The acute lymphoblastic leukemia image database for image processing, Proceedings - International Conference on Image Processing, ICIP, pp. 2045–2048, 2011, doi: https://doi.org/10.1109/ICIP.2011.6115881.

18. A. Fink, E. Hung, I. Singh, and Y. Ben-Neriah, Immunity in acute myeloid leukemia: Where the immune response and targeted therapy meet, European Journal of Immunology, vol. 52, no. 1, pp. 34–43, Jan. 2022, doi: https://doi.org/10.1002/EJI.202048945.
19. C. T. Basima and J. R. Panicker, Enhanced leucocyte classification for leukaemia detection, Proceedings - 2016 International Conference on Information Science, ICIS 2016, pp. 65–71, Feb. 2017, doi: https://doi.org/10.1109/INFOSCI.2016.7845302.
20. E. M. Senan and M. E. Jadhav, Techniques for the Detection of Skin Lesions in PH<Superscript>2</Superscript> Dermoscopy Images Using Local Binary Pattern (LBP), Communications in Computer and Information Science, vol. 1381 CCIS, pp. 14–25, Jan. 2020, doi: https://doi.org/10.1007/978-981-16-0493-5_2.
21. Yoshua. Bengio, Learning deep architectures for AI, p. 127, 2009, Accessed: Dec. 15, 2021. [Online]. Available: https://books.google.com/books/about/Learning_Deep_Architectures_for_AI.html?id=cq5ewg7FniMC
22. E. M. Senan, A. Alzahrani, M. Y. Alzahrani, N. Alsharif, and T. H. H. Aldhyani, Automated Diagnosis of Chest X-Ray for Early Detection of COVID-19 Disease, Computational and Mathematical Methods in Medicine, vol. 2021, 2021, doi: https://doi.org/10.1155/2021/6919483.
23. E. M. Senan, F. W. Alsaade, M. I. A. Al-Mashhadani, T. H. H. Aldhyani, and M. H. Al-Adhaileh, Classification of Histopathological Images for Early Detection of Breast Cancer Using Deep Learning, Journal of Applied Science and Engineering, vol. 24, no. 3, pp. 323–329, 2021, doi: https://doi.org/10.6180/JASE.202106_24(3).0007.
24. Deep learning methodology proposal for the classification of erythrocytes and leukocytes, pp. 129–156, Jan. 2021, doi: https://doi.org/10.1016/B978-0-12-822226-3.00006-4.
25. A. Alam and S. Anwar, Detecting Acute Lymphoblastic Leukemia Through Microscopic Blood Images Using CNN, Lecture Notes in Electrical Engineering, vol. 740 LNEE, pp. 207–214, 2021, doi: https://doi.org/10.1007/978-981-33-6393-9_22.
26. M. Ghaderzadeh, F. Asadi, A. Hosseini, D. Bashash, H. Abolghasemi, and A. Roshanpour, Machine Learning in Detection and Classification of Leukemia Using Smear Blood Images: A Systematic Review, Scientific Programming, vol. 2021, 2021, doi: https://doi.org/10.1155/2021/9933481.
27. B. A. Mohammed et al., Multi-Method Analysis of Medical Records and MRI Images for Early Diagnosis of Dementia and Alzheimer’s Disease Based on Deep Learning and Hybrid Methods, Electronics 2021, Vol. 10, Page 2860, vol. 10, no. 22, p. 2860, Nov. 2021, doi: https://doi.org/10.3390/ELECTRONICS10222860.
28. E. M. Senan, I. Abunadi, M. E. Jadhav, and S. M. Fati, Score and Correlation Coefficient-Based Feature Selection for Predicting Heart Failure Diagnosis by Using Machine Learning Algorithms, Computational and Mathematical Methods in Medicine, vol. 2021, pp. 1–16, Dec. 2021, doi: https://doi.org/10.1155/2021/8500314.
29. Z. Liu et al., A survey on applications of deep learning in microscopy image analysis, Computers in Biology and Medicine, vol. 134, p. 104523, Jul. 2021, doi: https://doi.org/10.1016/J.COMPBIOMED.2021.104523.